AEM
Journals.ASM.org

Potential Role of Nitrite for Abiotic Fe(II) Oxidation and Cell Encrustation during Nitrate Reduction by Denitrifying Bacteria

Nicole Klueglein,[a] Fabian Zeitvogel,[b] York-Dieter Stierhof,[c] Matthias Floetenmeyer,[d] Kurt O. Konhauser,[e] Andreas Kappler,[a] Martin Obst[b]

Geomicrobiology[a] and Environmental Analytical Microscopy,[b] Center for Applied Geosciences, University of Tuebingen, Tuebingen, Germany; Center for Plant Molecular Biology, University of Tuebingen, Tuebingen, Germany[c]; Max Planck Institute for Developmental Biology, Tuebingen, Germany[d]; Department of Earth and Atmospheric Sciences, University of Alberta, Edmonton, Alberta, Canada[e]

Microorganisms have been observed to oxidize Fe(II) at neutral pH under anoxic and microoxic conditions. While most of the mixotrophic nitrate-reducing Fe(II)-oxidizing bacteria become encrusted with Fe(III)-rich minerals, photoautotrophic and microaerophilic Fe(II) oxidizers avoid cell encrustation. The Fe(II) oxidation mechanisms and the reasons for encrustation remain largely unresolved. Here we used cultivation-based methods and electron microscopy to compare two previously described nitrate-reducing Fe(II) oxidizers (*Acidovorax* sp. strain BoFeN1 and *Pseudogulbenkiania* sp. strain 2002) and two heterotrophic nitrate reducers (*Paracoccus denitrificans* ATCC 19367 and *P. denitrificans* Pd 1222). All four strains oxidized ~8 mM Fe(II) within 5 days in the presence of 5 mM acetate and accumulated nitrite (maximum concentrations of 0.8 to 1.0 mM) in the culture media. Iron(III) minerals, mainly goethite, formed and precipitated extracellularly in close proximity to the cell surface. Interestingly, mineral formation was also observed within the periplasm and cytoplasm; intracellular mineralization is expected to be physiologically disadvantageous, yet acetate consumption continued to be observed even at an advanced stage of Fe(II) oxidation. Extracellular polymeric substances (EPS) were detected by lectin staining with fluorescence microscopy, particularly in the presence of Fe(II), suggesting that EPS production is a response to Fe(II) toxicity or a strategy to decrease encrustation. Based on the data presented here, we propose a nitrite-driven, indirect mechanism of cell encrustation whereby nitrite forms during heterotrophic denitrification and abiotically oxidizes Fe(II). This work adds to the known assemblage of Fe(II)-oxidizing bacteria in nature and complicates our ability to delineate microbial Fe(II) oxidation in ancient microbes preserved as fossils in the geological record.

Iron(II)-oxidizing bacteria play a significant role in geochemical element cycling and are involved in iron redox transformation under oxic, microoxic, and anoxic conditions in the environment (1–4). Their use of Fe(II) as electron donor at neutral pH leads to the formation of Fe(III) and rapid precipitation of poorly soluble Fe(III) (oxyhydr)oxide minerals. Besides affecting the iron cycle, Fe(III) minerals are important for transformation and immobilization of pollutants, heavy metals, and toxic metalloids (5–7). One physiological group of Fe(II) oxidizers, which has been studied extensively since its discovery in 1996, are nitrate-reducing Fe(II)-oxidizing bacteria (8). They use nitrate (NO_3^-) as well as intermediates or end products of denitrification and of dissimilatory nitrate reduction (NO_2^-, NO, and N_2O) (equation 1) as electron acceptors.

$$NO_3^- \longrightarrow NO_2^- \longrightarrow NO \longrightarrow N_2O \longrightarrow N_2 \qquad (1)$$

Most of the isolated strains grow mixotrophically and thus need an organic cosubstrate (e.g., acetate) for continuous Fe(II) oxidation and growth. Nitrate-reducing Fe(II)-oxidizing organisms have recently received a lot of attention because they seem to be widespread and abundant at neutral pH in anoxic habitats and belong to a variety of different bacterial phyla (2, 9–12). Nitrate-reducing iron-oxidizing bacteria and all other neutrophilic Fe(II) oxidizers face the problem of disposing of their poorly soluble metabolic product, i.e., Fe(III), at neutral pH. Rapid precipitation of Fe(III) minerals in the periplasm, on the cell surface, and in the immediate vicinity of the cell has been observed in microscopy studies with these Fe(II)-oxidizing microbes (13, 14). This can lead to the formation of a mineral crust around the cells that will probably hinder nutrient uptake and metabolite efflux, and thus metabolism, and may finally lead to cell death and lysis. In contrast, it has been shown that photoautotrophic and microaerophilic Fe(II) oxidizers are capable of avoiding encrustation. Different mechanisms to prevent encrustation have been postulated (15). First, low-pH microenvironments around the cells have been shown for phototrophic Fe(II)-oxidizing bacteria (16). Lowering the pH will increase the solubility of the formed Fe(III), which will be able to diffuse away from the cell surface before precipitating. Second, microaerophilic bacteria, such as *Gallionella* and *Leptothrix* species, are known for their production of organic structures that are attached to the outer cell surface. These so-called twisted stalks and sheaths capture and bind the Fe(III) as soon as it is produced, allowing the cell surface, periplasm, and cytoplasm to remain free of mineral encrustation (17–19). The production of organic fibers, which act as a template for mineral precipitation, have also been shown with phototrophic bacteria, such as *Rhodobacter* sp. strain SW2 (20). Third, Saini and Chan (21) showed a near-neutral cell surface charge and hydrophobicity for *Mariprofundus ferrooxydans* and *Gallionella* sp., which will decrease binding and precipitation of positively charged iron(III)

Received 1 October 2013 **Accepted** 19 November 2013
Published ahead of print 22 November 2013
Address correspondence to Andreas Kappler, andreas.kappler@uni-tuebingen.de.
Supplemental material for this article may be found at http://dx.doi.org/10.1128/AEM.03277-13.

doi:10.1128/AEM.03277-13

ions on the cell surface. Fourth, soluble organic ligands which can complex and solubilize Fe(III) have been proposed (15, 22). However, until now, no such molecules have been detected and identified in cultures of nonencrusted Fe(II)-oxidizing bacteria.

In contrast, nitrate-reducing Fe(II) oxidizers have as yet not been shown to prevent ferric iron encrustation in substrate-rich batch systems. Chakraborty et al., however, showed that *Acidovorax* sp. strain 2AN does not become encrusted when cultured in an advective system at low Fe(II) concentrations (50 to 250 μM) or with EDTA-chelated Fe(II) (12, 23). Cell encrustation has been demonstrated thoroughly with the mixotrophic *Acidovorax* strain BoFeN1 (10), for which minerals were shown to precipitate at the cell wall and within the periplasm (13–15, 24, 25). For instance, Miot et al. (24) observed the formation of Fe(III)-phosphate minerals within 30 min after inoculation of the Fe(II)-containing medium with BoFeN1 cells, ultimately leading to a thick mineral crust around the cells within 3 days. These differences observed for nitrate-reducing Fe(II) oxidizers compared to phototrophic and microaerophilic Fe(II) oxidizers raise the question of why some Fe(II)-oxidizing bacteria seem to have evolved efficient strategies to prevent encrustation, while some have not, despite living in similar geochemical conditions (26). One potential reason for the observed differences in Fe(III) mineral precipitation could be the role of abiotic versus biotic (enzymatic) Fe(II) oxidation under different incubation conditions. For the nitrate-reducing Fe(II) oxidizers, doubts have recently been expressed regarding the capability of anaerobic, enzymatic Fe(II) oxidation, suggesting an important contribution of abiotic Fe(II) oxidation by nitrite and NO (equations 2 to 5; vertical arrows indicate gaseous products) (27–29) and even questioning the capability of enzymatic Fe(II) oxidation (30).

$$2\,NO_2^- + 2\,H^+ \rightleftharpoons 2\,HNO_2 \longrightarrow NO_2\uparrow + NO\uparrow + H_2O \quad (2)$$

$$NO_2 + 2\,Fe^{2+} + 2H^+ \longrightarrow 2\,Fe^{3+} + NO\uparrow + H_2O \quad (3)$$

$$NO + Fe^{2+} + H^+ \longrightarrow Fe^{3+} + HNO\uparrow \quad (4)$$

$$2\,HNO \longrightarrow N_2O\uparrow + H_2O \quad (5)$$

In a recent study (31), we demonstrated experimentally that reactive nitrite, which is produced, for example, by strain BoFeN1 during nitrate reduction with electrons from acetate oxidation, plays a major role in abiotic Fe(II) oxidation in these cultures. This raises the question of whether the strains isolated originally as nitrate-reducing Fe(II) oxidizers have a specific enzymatic machinery for Fe(II) oxidation at all, or whether at least some if not all of the observed Fe(II) oxidation is abiotically driven.

Nitrate-reducing bacteria are often very abundant in soils and sediments, and they belong to a wide range of different phylogenetic groups (32). It is currently unknown whether abiotic Fe(II) oxidation as a consequence of bacterial nitrite production (in the presence of organic electron donors and ferrous iron) is a common phenomenon for denitrifiers. It is also unknown whether this abiotic Fe(II) oxidation process may lead to encrustation of these denitrifying cells comparable to that observed for the described nitrate-reducing Fe(II) oxidizers. Therefore, in this study, we compared Fe(II) oxidation and cell encrustation in four different bacterial strains capable of heterotrophic nitrate reduction. Two strains were isolated and described as nitrate-reducing Fe(II) oxidizers: the mixotrophic *Acidovorax* strain BoFeN1 and *Pseudogulbenkiania* strain 2002, a strain that was described as being able to grow lithoautotrophically with Fe(II) and nitrate (11, 33). The two other strains are well-characterized, heterotrophic, denitrifying bacteria: *Paracoccus denitrificans* strains Pd 1222 (34) and ATCC 19367 (35). We cultivated all four strains in the presence of nitrate, acetate (as an organic electron donor), and ferrous iron to determine whether there is Fe(II) oxidation, nitrite accumulation, and cell encrustation.

MATERIALS AND METHODS

Source of microorganisms. Strain BoFeN1 was isolated from Lake Constance sediments (10) and had been kept in the authors' laboratory since its original isolation. *Pseudogulbenkiania* strain 2002 was isolated from a freshwater lake in Illinois (11) and was purchased from the DSMZ, Germany. *Paracoccus denitrificans* was first isolated by Beijerinck in 1910 from soil (36). *Paracoccus denitrificans* ATCC 19367 and *P. denitrificans* Pd 1222 were generously provided by Sebastian Kopf, California Institute of Technology.

Microbial growth medium and growth conditions. For routine cultivation, all strains were grown in 22 mM bicarbonate-buffered low phosphate mineral medium (pH 7.1), which was prepared anoxically as described in detail by Hegler et al. (37). *Acidovorax* strain BoFeN1 and *Pseudogulbenkiania* 2002 were cultivated with 10 mM sodium nitrate and 5 mM sodium acetate. Both *Paracoccus denitrificans* strains were cultivated with 10 mM sodium nitrate and 5 mM sodium succinate.

Experimental setup. For oxidation experiments, 8 mM Fe(II)-containing medium was prepared as described by Klueglein and Kappler (31). Bottles were amended with anoxic sodium nitrate (10 mM) and sodium acetate (5 mM) and inoculated with 5% (vol/vol) of a four-day-old preculture grown on 5 mM acetate and 10 mM nitrate (optical density at 600 nm [OD_{600}] = 0.22). Sterile set-ups were used as controls. All cultures were incubated at 28°C in the dark. Growth experiments were conducted in duplicate; both values are presented to illustrate the variation of the data.

Analytical methods. For quantification of Fe(II) and Fe(III), we used the revised ferrozine protocol for nitrite-containing samples provided by Klueglein and Kappler (31). Briefly, 100 μl of culture suspension was withdrawn anoxically with a syringe and dissolved in 900 μl of 40 mM sulfamic acid for 1 h at room temperature. Sulfamic acid reacts with the nitrite present and therefore prevents abiotic oxidation of Fe(II) by reactive N species formed during sample acidification. The purple ferrozine-Fe(II) complex was quantified at 562 nm using a microtiter plate reader (FlashScan 550; Analytik Jena, Germany). Ferrozine measurements were done in triplicate. Maximum rates of microbial iron oxidation for the cultures were calculated from the steepest slope between two subsequent data points of Fe(II) concentrations. Acetate was quantified by high-performance liquid chromatography (HPLC) (class VP with RID 10 A and DAD SPM 10A VP detectors [Shimadzu, Japan]; the precolumn was a Microguard cation H cartridge; the main column was an Aminex HPX-87H ion exclusion column [300 mm by 7.8 mm] [Bio-Rad, Austria]; eluent, 5 mM H_2SO_4 in MQ water). For quantification of cell growth in Fe(II)-free cultures (acetate/nitrate only), optical density (OD) was quantified at 600 nm (SPEKOL 1300; Analytik Jena, Germany). Nitrate and nitrite were quantified by a continuous-flow analyzer system containing a dialysis membrane for iron removal to prevent side reactions during analysis (Seal Analytical, Norderstedt, Germany). In this automated system, nitrate is reduced to nitrite with hydrazine sulfate and quantified photometrically with *N*-1-naphtylethylendiamin at 550 nm. Minerals were identified with a micro-X-ray-diffraction (XRD) device (Bruker D8 Discover X-ray diffraction instrument; Bruker AXS GmbH, Germany) equipped with a Co K_α X-ray tube and operating at 30 kV and 30 mA (38). The EVA 10.0.1.0 software was used to identify the containing mineral phases using the PDF database licensed by ICDD (International Centre for Diffraction Data).

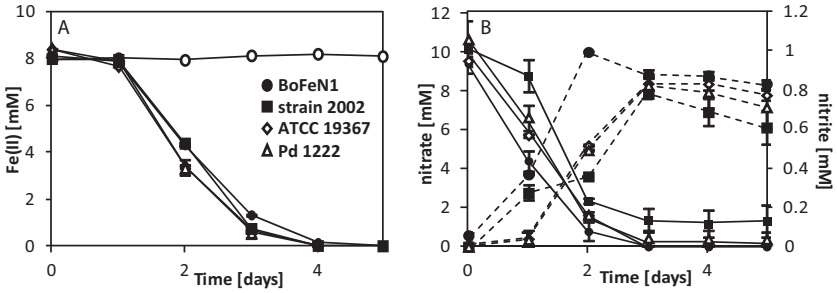

FIG 1 Oxidation of Fe(II), nitrate consumption, and nitrite formation by four nitrate-reducing strains. (A) Total Fe(II) concentrations over time for *Acidovorax* strain BoFeN1, *Pseudogulbenkiania* strain 2002, *Paracoccus denitrificans* ATCC 19367, *Paracoccus denitrificans* Pd 1222, and a sterile control (○). (B) Dissolved concentrations of nitrate (solid lines) and nitrite (dashed lines) for the four tested strains. Sterile controls showed neither a decrease in nitrate nor an increase in nitrite (data not shown). Error bars indicate the ranges for two parallel determinations. The absence of error bars indicates that the error bar is smaller than the symbol.

Electron and fluorescence microscopy. After Fe(II)-oxidizing experiments had run to completion (6 days), the cells were prepared for electron microscopy imaging. For scanning electron microscopy (SEM), cells from iron-containing cultures were fixed with 2.5% glutaraldehyde at 4°C overnight. The samples were applied to poly-L-lysine-coated glass coverslips, washed with PBS, and successively dehydrated using a series of ethanol dilutions (30%, 70%, 95%, and 100% [twice], dried on a molecular sieve). After critical-point drying in CO_2, the samples were mounted on SEM stubs using conductive carbon pads. Since the thin samples were sufficiently conductive to avoid major charge effects, the samples were not coated to preserve maximum Z contrast. The samples were examined with a LEO 1450 VP at 5 kV for secondary electron (SE) contrast, showing the cell surfaces, or 12 kV for backscattered electron (BSE) contrast, showing the distribution of Fe at the surface of and within the bacteria. Being dominated by topography contrast, SE images show the topographic structure of the samples, with only a minor influence of their chemical composition. In contrast, BSE images are characterized by Z-number contrast, resulting in higher brightness from areas with a higher average atomic number. This allowed the identification of Fe accumulations within the organic samples. Thus, it was possible to obtain information on both the surface of the samples that was shown in SE images and the distribution of iron visible in BSE images.

For transmission electron microscopy (TEM), cells from six-day-old iron-containing cultures were centrifuged and picked up with cellulose capillaries with a diameter of 200 μm. These were immediately submersed in 1-hexadecene. The capillaries were cut into segments approximately 2 mm in length that fit precisely into the cavity of standard aluminum platelets (depth, 150 μm) for high-pressure freezing filled with 1-hexadecene. The platelets were sandwiched with a second platelet without cavity and high-pressure frozen using an HPM 010 high-pressure freezer (Bal-Tec, Lichtenstein). The frozen samples were freeze-substituted in 1.25% glutaraldehyde in acetone using a Leica EMAFS freeze substitution unit. The temperature was kept at −90°C for 40 h, raised to −60°C over 6 h, kept at −60°C for 4 h, raised to −40°C over 4 h, raised to 0°C over 2 h, and kept at 0°C for 1 h. Subsequently, the samples were washed five times in acetone and embedded in Epon, infiltrating them with 10% Epon resin in acetone for 2 h, 25% Epon overnight, 50% Epon for 8 h, 75% Epon overnight, 100% Epon for 8 h, and 100% Epon for 20 h, before being placed in embedding molds containing fresh resin and polymerized at 60°C for 2 days. Ultrathin sections with a nominal thickness of 70 nm were prepared on an Om U3 ultramicrotome (C. Reichert, Austria) using a diamond knife (DuPont Instruments) and placed on Formvar-coated 300-mesh Cu TEM grids (Plano, Wetzlar, Germany). TEM images were acquired using a FEI Tecnai Spirit G^2 TEM equipped with a Biotwin lens and operated at 120 kV. For measurement of the width of the extracellular polymeric substance (EPS) envelope, the distance between cell surface and iron minerals was measured at three different positions per cell in at least 10 individual cells. To show and compare the variability of the data, the standard deviations of all measurements are presented.

For fluorescence microscopy, samples were stained with wheat germ agglutinin (WGA) Alexa Fluor 633 conjugate, targeting extracellular polymeric substances (EPS) (39) (Invitrogen, Carlsbad, CA) for 20 min and rinsed three times. Images were acquired using a Leica DM 6000 epifluorescence microscope equipped with a 63× air lens with a numerical aperture (NA) of 0.9 and a DFC360 FX camera. The Alexa dye was excited with red light while far-red fluorescence was recorded. Confocal laser scanning microscopy (CLSM) images were acquired using a Leica SPE system and an ACS APO 63× lens (NA = 1.15). For CLSM imaging, DNA was stained with Syto 9 (Invitrogen, Carlsbad, CA), lipids were stained with FM4-64 (Invitrogen, Carlsbad, CA), and EPS was stained with a WGA-Alexa Fluor 555 conjugate (Invitrogen, Carlsbad, CA). The excitation laser wavelengths were 488 nm, 561 nm, and 561 nm, whereas the recorded emission ranges were 492 to 520 nm, 570 to 650 nm, and 710 to 800 nm, respectively. Minerals were recorded using their reflection signal of the 488-nm laser.

RESULTS

Fe(II) oxidation, nitrate reduction, and nitrite accumulation. *Acidovorax* strain BoFeN1, *Pseudogulbenkiania* strain 2002, *Paracoccus denitrificans* ATCC 19367, and *Paracoccus denitrificans* Pd 1222 were cultivated in the presence of ~8 mM dissolved Fe(II), 10 mM nitrate (NO_3^-) and 5 mM acetate. All strains oxidized Fe(II) to completion within 4 days at similar maximum rates (BoFeN1, 3.6 ± 0.0 mM/day; 2002, 3.6 ± 0.1 mM/day; ATCC 19367, 4.3 ± 0.1 mM/day; Pd 1222, 4.5 ± 0.3 mM/day) (Fig. 1A). [Similar Fe(II) oxidation rates for strain BoFeN1 and strain 2002 were published before (11, 31).] Although the four strains showed very similar Fe(II) oxidation trends over time, nitrate reduction and nitrite accumulation differed slightly between the strains. BoFeN1 accumulated up to 1 mM nitrite at day 2 and consumed all available nitrate and all available acetate within 3 to 4 days (Fig. 1B and Fig. 2). Strain 2002 accumulated slightly less nitrite (~0.4 mM) at day 2 and also consumed all provided acetate but did not reduce all available nitrate [remaining nitrate concentration was ca. 1.4 mM after 5 days when all Fe(II) and acetate was already consumed; incomplete nitrate reduction was also observed by Weber et al. (11)]. Both *Paracoccus denitrificans* strains showed very similar and complete nitrate consumption and nitrite production of up to 0.8 mM. Nitrite accumulation in both cultures started at day 1 and reached the maximum concentration at day 3.

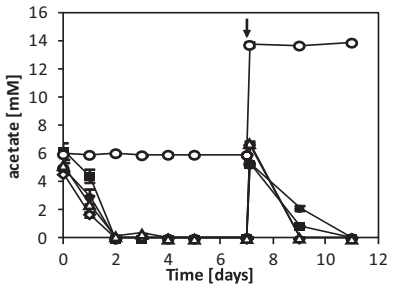

FIG 2 Acetate consumption during incubation with 10 mM nitrate and ~8 mM Fe(II) over time for *Acidovorax* strain BoFeN1 (●), *Pseudogulbenkiania* strain 2002 (■), *Paracoccus denitrificans* ATCC 19367 (◇), *Paracoccus denitrificans* Pd 1222 (△), and a sterile control (○). The arrow indicates the spike with ~5 mM acetate and ~10 mM nitrate at day 7 after all acetate had been consumed. Error bars indicate the ranges for two parallel determinations. The absence of error bars indicates that the range was smaller than the symbol.

Acetate was already consumed completely at day 2, similar to cultures of strain BoFeN1 and strain 2002 (Fig. 2).

Encrustation of cells during Fe(II) oxidation. Using both secondary electron (SE) and backscattered electron (BSE) imaging on the SEM, we characterized the distribution of Fe(III) minerals at the cell surface and within the periplasm. Figure 3A and B show cells of strain BoFeN1 grown in the presence of Fe(II) and, therefore, associated with iron(III) minerals. Some cells have minerals with needle-like structures on their surfaces (Fig. 3A, arrow 2 and inset), whereas other cells seem to retain smooth surfaces. When BSE contrast is used, the iron minerals can be clearly distinguished from the cells, which show some iron inside the periplasm, resulting in a bright rim structure around the cells on the BSE images (Fig. 3B, arrow 3). Nonencrusted cells (Fig. 3A and B, arrow 1) were almost invisible in BSE mode. Compared to BoFeN1, *Pseudogulbenkiania* strain 2002 showed smaller mineral agglomerates with a globular shape (~40 nm) but no needle-shaped minerals (Fig. 3C). One of the cells appears very bright in the corresponding

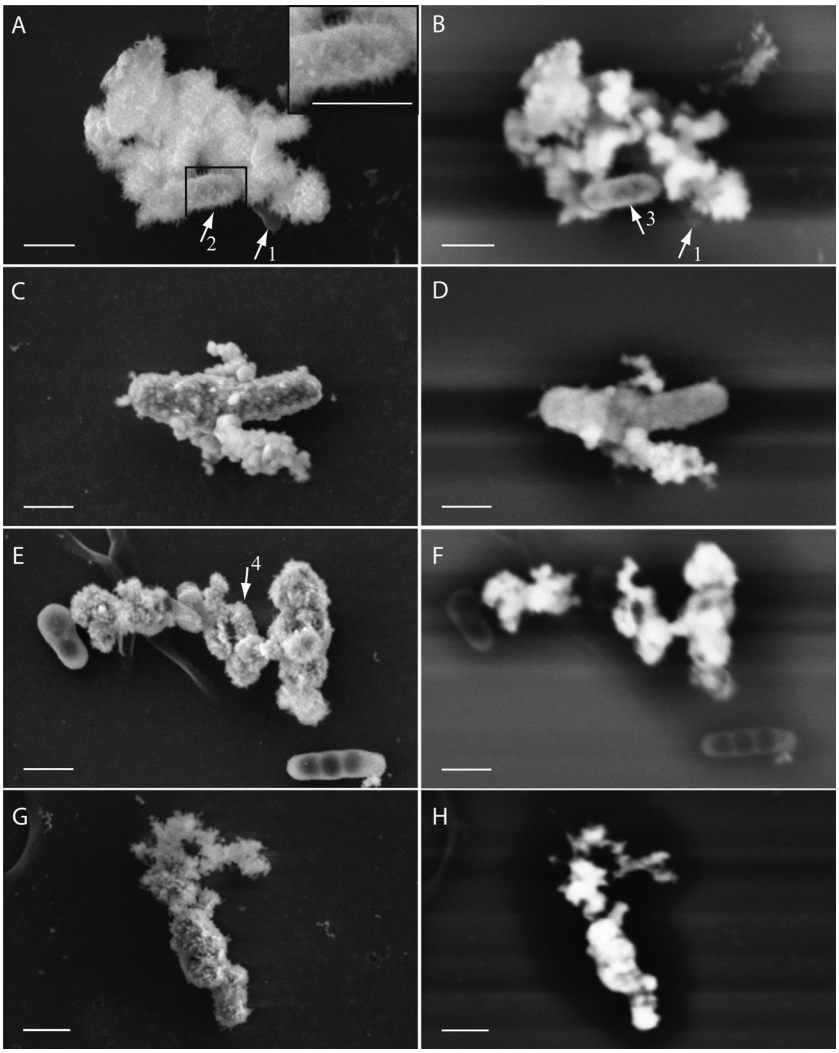

FIG 3 SEM images of four nitrate-reducing strains cultured in the presence of 10 mM nitrate, 5 mM acetate, and ~8 mM Fe(II). SE (5 kV) (left) and BSE (10 to 12 kV) (right) images of samples of bacterial strains *Acidovorax* strain BoFeN1 (A and B), *Pseudogulbenkiania* strain 2002 (C and D), *Paracoccus denitrificans* ATCC 19367 (E and F), and *Paracoccus denitrificans* Pd 1222 (G and H) are shown. Arrows 1 point to a nonencrusted cell of strain BoFeN1. Arrow 2 points to needle-like minerals. Arrow 3 points to the encrusted periplasm of a cell. Arrow 4 points to a complete encrusted cell. Bars, 500 nm.

BSE image (Fig. 3D), indicating a strong internal accumulation of iron. The cells of *Paracoccus denitrificans* strain ATCC 19367 appear smooth in SE mode but show at least some iron accumulation inside the periplasm (Fig. 3E and F). Some of the visible structures can be interpreted as fully encrusted cells (Fig. 3E, arrow 4). Strain Pd 1222 shows needle- and plate-shaped minerals on the surface along with a strong BSE signal that can be attributed to strong periplasmic or cytoplasmic Fe accumulations (Fig. 3G and H).

To confirm these observations made by SEM, we prepared high-pressure frozen and freeze-substituted samples from fully oxidized cultures for TEM imaging without addition of heavy metal stains to allow undisturbed imaging of the iron mineral distribution and to minimize preparation artifacts. As a consequence, contrast in the TEM is mainly caused by iron(III) minerals, while organic structures create minimal or no contrast. *Acidovorax* strain BoFeN1 cells showed several encrustation patterns (Fig. 4A and B; also, see Fig. S1 in the supplemental material). First, one fraction of cells showed cauliflower-like structures in direct contact with or distant from the cells (Fig. 4A), suggesting that these cells excreted extracellular compounds which bound Fe(III) or acted as nucleation sites. Second, in some cells, not only was there a mineral layer within the periplasm, but also the cytoplasm was to a large extent filled with iron minerals (see Fig. S1 in the supplemental material). Third, in some cells, encrustation was characterized by mineral plates several hundred nanometers in size on the cell surface, sometimes surrounding the entire cell (Fig. 4B, arrow 1). The cytoplasm did not appear to be fully mineralized, despite the fact that the mineral plates seemed to originate from inside the periplasmic membrane. Fourth, some cells were free of mineral precipitates except for their periplasm (Fig. 4B, arrow 2). In contrast to the variety of encrustation patterns observed for BoFeN1, the other three strains showed a more uniform behavior. The cells of *Pseudogulbenkiania* strain 2002 were mostly filled with regularly shaped Fe(III) minerals (Fig. 4C and D) which were in most cases smaller than those observed for BoFeN1 (Fig. 4A and B). All cells of strain 2002 were enclosed by a capsule of very fine-grained Fe(III) minerals that were either in direct contact with the cell surface or in close proximity (Fig. 4C). Very few cells showed a slightly encrusted periplasm without internal or external minerals (Fig. 4D, arrow 3). *Paracoccus denitrificans* ATCC 19367 (Fig. 4E and F) showed encrustation patterns similar to those of Pd 1222 (Fig. 4G and H). For a large number of cells, the cytoplasm was completely filled with large, crystalline Fe(III) mineral particles. Many cells were enclosed by shells composed of Fe(III) mineral plates of ~100 nm that were not in direct contact with the cell surface but separated by a thick, non-electron-dense layer. This is probably the result of excretion of EPS, which also seems responsible for connecting the cells into chains and aggregates (Fig. 4F). XRD analysis of the mineral products of all tested strains showed diffraction reflexes indicative of goethite (see Fig. S2 in the supplemental material).

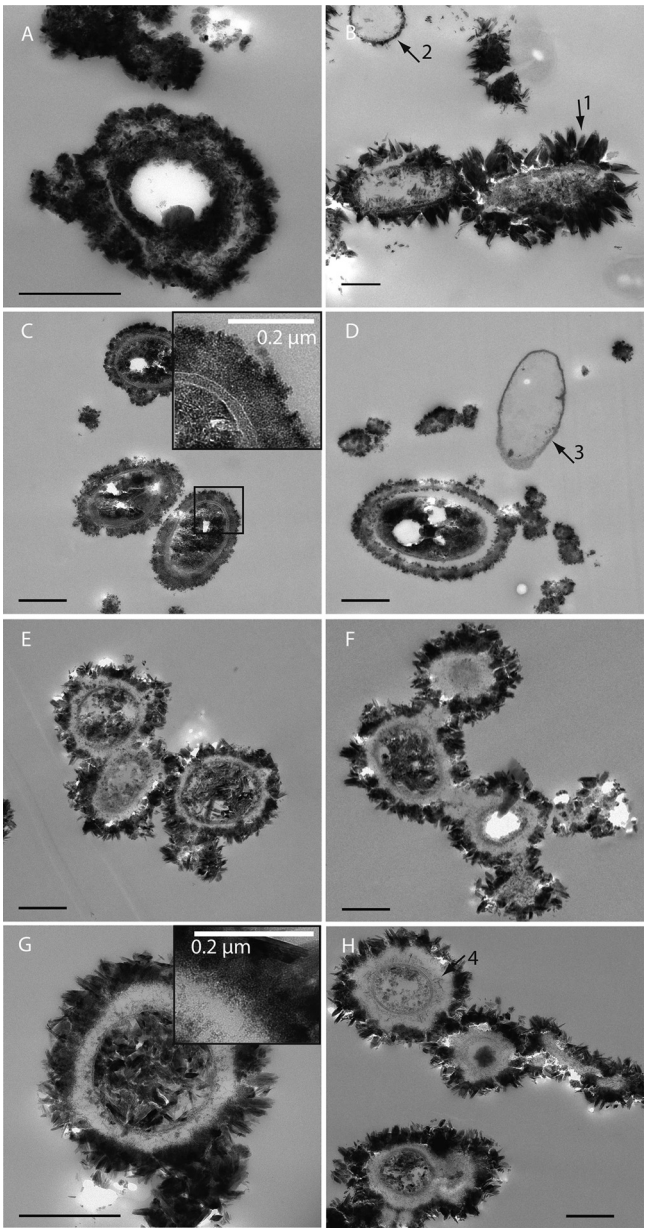

FIG 4 Resin sections (TEM images) of cryofixed and freeze-substituted *Acidovorax* strain BoFeN1 (A and B), *Pseudogulbenkiania* strain 2002 (C and D), *Paracoccus denitrificans* ATCC 19367 (E and F), and *Paracoccus denitrificans* Pd 1222 (G and H). Cells were cultivated in the presence of 10 mM nitrate, 5 mM acetate, and ~8 mM Fe(II). Arrow 1 points to mineral plates surrounding a BoFeN1 cell. Arrow 2 points to a BoFeN1 cell with encrusted periplasm. Arrow 3 points to a 2002 cell with encrusted periplasm. Arrow 4 points to filamentous structures inside the EPS. Cells are not stained. Bars, 500 nm (unless stated otherwise).

EPS formation by nitrate-reducing cells in the presence and absence of Fe(II). To identify EPS in the surrounding of the cells, we stained ultrathin sections of all four strains on TEM grids with the EPS-binding lectin WGA conjugated with Alexa Fluor 633. Using epifluorescence, we observed bright fluorescence in the cell rims for all Fe(II)-grown cultures, clearly indicating the presence of EPS (Fig. 5A; also, see Fig. S3 in the supplemental material). The strongest signal was detected for the *Paracoccus denitrificans* Pd 1222 cells (Fig. 5A). Even larger amounts of EPS might have been present in native samples but could potentially have been extracted before analysis as a consequence of exposure to acetone during TEM sample preparation. When analyzing wet samples of BoFeN1 by CLSM, we observed a very pronounced EPS envelope around the cells cultured with Fe(II), but with the same lectin, no fluorescence was detectable in iron-free samples (Fig. 6).

Visualizing a cell profile with additional staining of cell membrane lipids clearly shows that the Fe(II)-grown cells are actually

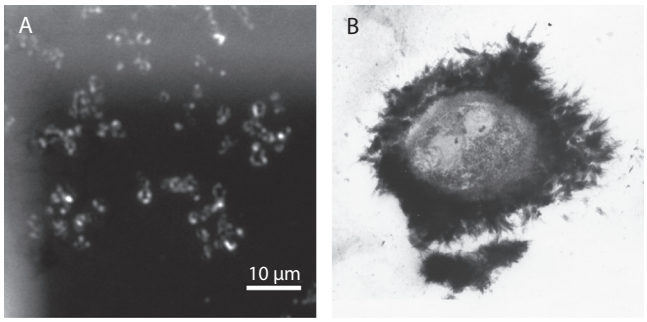

FIG 5 (A) Fluorescence image of *Paracoccus denitrificans* Pd 1222 grown in the presence of Fe(II). EPS was stained with WGA-Alexa Fluor 633 conjugate directly on TEM grids. Bright color indicates the fluorescing EPS shells. (B) TEM image of iron oxide precipitation around an encapsulated bacterium in a thin section collected at 432 m underground at the Äspö Hard Rock Laboratory near Oskarshamn, Sweden. The sample was stained with uranyl acetate to enhance the electron contrast of the biological material.

surrounded by EPS (see Fig. S4 in the supplemental material). Analysis of the thickness of the surrounding layers from TEM images showed that Pd 1222 has the most pronounced EPS envelope (253 ± 53 nm), in contrast to strain 2002, which showed the thinnest EPS envelope (109 ± 28 nm). In the EPS layers of Pd 1222 and ATCC 19367, electron-dense filamentous structures can be observed (Fig. 4G, inset, and H, arrow 4), which are likely accumulations of Fe(III). At the outer layer of the EPS, particles in the nanometer size range form, which might act as nucleation sites, leading to bigger iron mineral crystals. In contrast to the cytoplasm, which is filled with large and very crystalline mineral particles, in the *Paracoccus* cultures we observed very small and poorly crystalline Fe(III) mineral particles inside the EPS-rich layer, where the growth of larger crystals seems to be inhibited by the EPS (Fig. 4G, inset). In contrast to strain BoFeN1 and the *Paracoccus* strains, strain 2002 seems to form much smaller Fe(III) mineral particles (in the nanometer range), which are visible as a very electron-dense and compact layer around the cell (Fig. 4C and D). At the outer edge of the EPS-iron layer of strain 2002, slightly larger Fe(III) mineral particles are visible (Fig. 4C, inset).

Acetate consumption by encrusted cells after complete Fe(II) oxidation. The formation of large amounts of poorly soluble Fe(III) minerals at the cell surface and in the cell interior raises the question of whether these cells can actually maintain their metabolic activity or whether the cell encrustation slows down metabolic activity or even leads to cell lysis. To answer this question, we followed acetate consumption of all four cultures over time (Fig. 2). We found that all four strains consumed the initially present 5 mM acetate within approximately 2 days, when 8 to 23% (0.8 to 2.3 mM) of the provided nitrate was still in solution. After complete consumption of acetate and complete Fe(II) oxidation, we spiked the cultures again with 5 mM acetate and 10 mM nitrate at day 7. We found that all four strains were able to resume acetate consumption (BoFeN1, 1.6 ± 0.1 mM/day; 2002, 2.3 ± 0.0 mM/day; ATCC 19367, 3.5 ± 0.1 mM/day; Pd 1222, 3.5 ± 0.1 mM/day, respectively) even at this late stage of encrustation, indicating that at least some cells were still metabolically active.

DISCUSSION

Of the four strains used in our study, two were isolated as nitrate-reducing Fe(II) oxidizers, while the other two were known to be ordinary denitrifiers. All four strains not only caused oxidation of Fe(II) but also were encrusted with Fe(III) minerals during Fe(II) oxidation. Although the observed encrustation patterns differed slightly, the four strains behaved similarly regarding Fe(II) oxidation rate and extent, nitrate consumption, nitrite accumulation, and identity and localization of Fe(III) minerals. Overall, our data show that Fe(II) oxidation under denitrifying conditions in the presence of high substrate concentrations can be caused by many more bacteria than previously thought. In particular, Fe(II) oxidation can also be induced by bacteria that probably do not contain an enzymatic system for Fe(II) oxidation. With this study, we also want to draw attention to the possible abiotic side reactions of

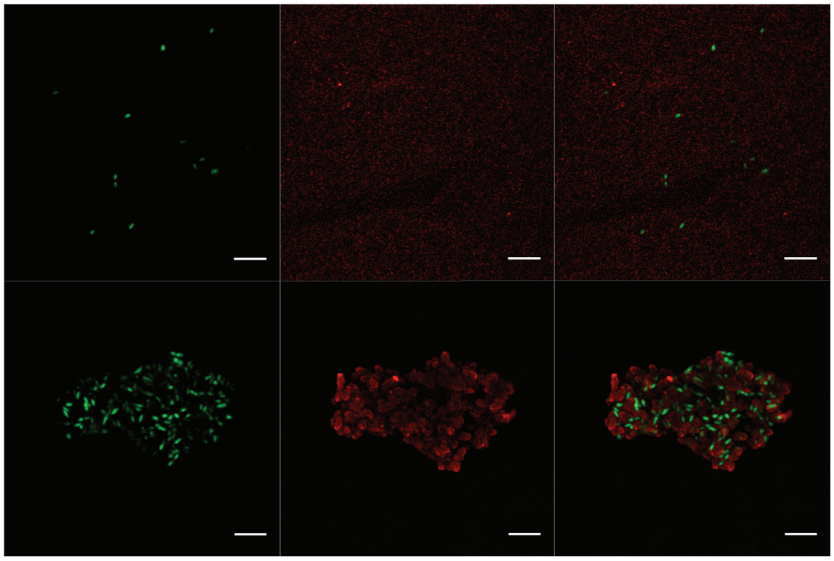

FIG 6 CLSM images of *Acidovorax* strain BoFeN1 incubated for 7 days with 10 mM nitrate and 5 mM acetate and without Fe(II) (top) and with ~8 mM Fe(II) (bottom). DNA was stained with Syto9 (green), and EPS was stained with WGA-Alexa Fluor 555 conjugate (red). Images on the right show the overlay of both images. Bars, 5 μm.

nitrite in these cultures, which have often not been taken into consideration, and also the fact that under anoxic conditions, Fe^{2+} seems to be toxic to the bacteria. This will help to better understand and evaluate anaerobic Fe(II) oxidation in natural environments.

Indirect abiotic Fe(II) oxidation by heterotrophic nitrate-reducing bacteria. Our data showed that the two denitrifying *Paracoccus* strains investigated efficiently oxidize Fe(II) when provided with nitrate, Fe(II), and acetate. Oxidation of Fe(II) by heterotrophic denitrifying *Paracoccus* strains has been tested before, with slightly different results. While Muehe et al. (40) found that *Paracoccus denitrificans* strain ATCC 17741 was also able to oxidize Fe(II) at low rates when the Fe(II) was added as $FeSO_4$ to the medium, Kumaraswamy et al. (41) observed no oxidation of dissolved Fe(II) but oxidation of chelated Fe(II) with ethanol as the carbon source by *Paracoccus denitrificans* strain NCCB 80056. To potentially resolve this discrepancy, we tested two additional *P. denitrificans* strains, i.e., *Paracoccus denitrificans* ATCC 19367 (35) and *Paracoccus denitrificans* Pd 1222 (a genetic modification of DSM 413^T) (34). We found that the two *Paracoccus* strains used in our study behaved very similarly to each other and that oxidation of dissolved, nonchelated Fe(II) was comparable to Fe(II) oxidation by the Fe(II) oxidizers *Acidovorax* strain BoFeN1 (10) and *Pseudogulbenkiania* strain 2002 (11, 33) (Fig. 1). Possible explanations for the differences between our study and the previous studies with *Paracoccus* strains that did not show Fe(II) oxidation could be the presence or absence of enzymatic Fe(II) oxidation in the different *Paracoccus* strains used and, which we believe is more likely, strain-specific physiological differences. Specifically, acetate oxidation and nitrate reduction resulted in differences in nitrite formation and thus different extents of abiotic Fe(II) oxidation and cell encrustation. The intricacies of this metabolism are illustrated by the available data for Fe(II) oxidation, nitrate consumption, and nitrite formation for strain BoFeN1 from several recent publications (10, 31, 40). These studies showed that small variations in cultivation conditions [e.g., preculture conditions, small pH differences, and different nitrate/acetate/Fe(II) concentrations and ratios] can lead to major differences in cell growth, substrate consumption, nitrite formation, and Fe(II) oxidation. Since in our study the concentrations of nitrate, carbon source, and Fe(II) were similar for all four strains tested, our study allowed a direct comparison of Fe(II) oxidation by four nitrate-reducing strains.

Nitrite accumulated in all four cultures (0.8 to 1 mM), although it has to be considered that this is only the remaining nitrite and does not take into account nitrite which had probably already reacted with Fe(II) or was further reduced to NO, N_2O, or N_2 and is, therefore, not included in the analysis. Nitrite accumulation, nitrate consumption, and concentrations of reacted nitrogen (see Fig. S5 in the supplemental material) differed slightly in the four tested strains. Despite these small differences, overall the Fe(II) oxidation rates were very similar in the four bacterial cultures (3.6 to 4.5 mM/day) when the strains were cultivated with an additional organic electron donor (Fig. 1A). These rates are similar to or slightly higher than abiotic Fe(II) oxidation rates (0.2 to 3.7 mM/day) (31). Cell surface catalysis was ruled out in a control experiment (see Fig. S6 in the supplemental material). Our data in combination with the recent literature provide strong evidence for the role of abiotic oxidation of Fe(II) by nitrite and NO in our cultures even at neutral pH (42–45). This reaction can be enhanced by reactive surfaces of the minerals formed, i.e., goethite and green rust, which was shown to be the main precursor mineral for goethite formation via a reaction with nitrite (46–49). Furthermore, it has been shown that strain BoFeN1 cannot couple N_2O reduction to Fe(II) oxidation, suggesting the absence of an enzymatic system for Fe(II) oxidation at least for strain BoFeN1 (31). Evidence for an enzymatic Fe(II) oxidation was provided by Chakraborty and Picardal (23), who found that Fe(II) oxidation is inducible at an enzymatic level for *Acidovorax* strain 2AN. In contrast, Carlson et al. (50) did not see inducible Fe(II) oxidation for *Acidovorax ebreus* strain TPSY, and in a proteomic study with the same strain, those authors did not find any specific proteins responsible for Fe(II) oxidation. Although the main question therefore still remains whether in these strains Fe(II) oxidation may be caused partly or even completely by an abiotic reaction with nitrite/NO, our present study showed that ordinary nitrate-reducing bacteria show nitrite accumulation and Fe(II) oxidation rates similar to those of two nitrate-reducing strains that were isolated as Fe(II) oxidizers. This suggests that under our chosen experimental conditions with relatively high substrate concentrations, the observed Fe(II) oxidation is, at least to a certain extent, indirect and caused by reactive nitrite/NO produced biologically from nitrate reduction with electrons stemming from provided or cell-stored acetate. Of course, this does not rule out the possibility that the *Paracoccus* strains used here or other nitrate-reducing Fe(II) oxidizers do have proteins for enzymatic Fe(II) oxidation and that at least some fraction of the observed oxidation could be enzymatically driven. This is in particular true for strain 2002, since this organism was described as being able to oxidize Fe(II) lithoautotrophically. However, although strain 2002 is capable of growing with Fe(II) as the sole electron donor and fixing CO_2 into organic carbon under nitrate reducing conditions, it cannot be indefinitely cultivated under lithoautotrophic conditions with Fe(II), and the metabolic pathway remains unknown (Karrie Weber, personal communication).

Variation in iron(III) mineral encrustation for different nitrate-reducing strains and for different cells within the same culture. The formation of mineral crusts around the cells during Fe(II) oxidation by nitrate-reducing Fe(II) oxidizers has been recognized before (10, 51) and was studied intensively with the mixotrophic bacterial strain *Acidovorax* strain BoFeN1 (10, 13–15, 24, 25). In the present study, we used SEM (Fig. 3) and TEM (Fig. 4; also, see Fig. S1 in the supplemental material) and identified different patterns of encrustation, including only a mineral-filled periplasm (Fig. 3B, arrow 3, and Fig. 4B, arrow 2), additional encrustation of the cell surface (Fig. 4B, arrow 1), and a fully mineralized cytoplasm (e.g., see Fig. S1 in the supplemental material). After complete Fe(II) oxidation, these different mineralization stages were found simultaneously in the same BoFeN1 culture. Previous studies with BoFeN1 described similar encrustation but reported additional globular structures rich in organic carbon on the cell surface (14, 15), while we observed needle- or plate-shaped goethite minerals (Fig. 3A and 4B). (For comparison to abiotic synthesized goethite, see reference 52.) We interpret these different patterns as a continuum of progressive mineralization stages resulting from different efficiencies (i.e., rates and time course) in nitrate reduction and nitrite formation of single cells depending on the iron, acetate, nitrate, and nutrient contents of the cultures and thus the metabolic state of the cells over time (53).

No data regarding encrustation have previously been pub-

lished for the nitrate-reducing Fe(II) oxidizer *Pseudogulbenkiania* strain 2002 or for heterotrophic denitrifiers such as *Paracoccus denitrificans*. The three strains of these species investigated here showed a similar and homogeneous encrustation behavior, i.e., massive encrustation, and many of the cells were completely filled with Fe(III) minerals (Fig. 4C to H), similar to some BoFeN1 cells. The Fe(III) mineral particles in the culture of strain 2002, however, remained smaller (only a few nanometers) (Fig. 4C and D) than those of BoFeN1, while the Fe(III) mineral particles in the *Paracoccus* cultures had a size of hundreds of nanometers both inside and outside the cells (Fig. 4E to H). This difference in particle size might hint at a different oxidation behavior in strain 2002. This could be caused by a different nitrite production rate (Fig. 1B) or transport or a difference in produced EPS, but also, the involvement of enzymatic Fe(II) oxidation cannot be ruled out, particularly since strain 2002 can grow lithoautotrophically on Fe(II) at least for some generations. However, the encrustation of all tested nitrate-reducing bacteria during growth in Fe(II)-rich medium further supports our hypothesis that nitrite is probably an important (abiotic) oxidant for Fe(II) in these strains and was responsible for the observed mineral formation and cell encrustation. We want to point out that cell encrustation might be also caused by the relatively high substrate concentrations typically used in batch cultures for Fe(II) oxidizers favoring heterotrophic nitrate reduction (24, 50, 54). It is possible that in the environment, where the concentrations are mostly much lower, cell encrustation is not as pronounced or even absent, as proposed by Chakraborty et al. (12). Future studies with continuous-flow experiments with low and thus more environmentally relevant Fe(II) and nitrate concentrations will show whether cell encrustation in these strains is mainly an artifact caused by batch experiments with high substrate concentrations.

EPS formation and possible influence on mineral formation. A noticeable feature in all four strains was the presence of shells of different diameters containing small mineral particles that enclosed the cells, forming a rim of up to 250 nm between the larger mineral particles and the cell surfaces (Fig. 4G). The WGA-binding study using the fluorescence microscope confirmed the presence of EPS with a shape resembling that of those shells (Fig. 5A; also, see Fig. S3 in the supplemental material). The EPS could be secreted by the cells either (i) in an attempt to protect the cell surface from encrustation or (ii) to bind toxic Fe^{2+}. The large mineral particles outside this EPS layer, especially in cultures of Pd 1222 and ATCC 19367 (Fig. 4E to H), seem to originate from a thin, electron-dense, and nanometer-size grained mineral layer at the outer rim of the EPS capsule. The organic EPS polymers likely block kinks and steps of the initially formed mineral nuclei and thus prevent the formation of larger crystals within the EPS layer (55). We indeed observed that the minerals within the capsule, visible as filamentous structures, were generally much smaller grained than those on the surface. This feature is most notable for Pd 1222 and ATCC 19367 (Fig. 4G, inset, and 4H, arrow 4), where minerals outside the EPS layer achieve sizes of several hundred nanometers while those within the EPS layer are merely nanometer-sized; similar observations have been made previously for other iron minerals nucleating within EPS in environmental samples (56). Strain 2002 differs in its encrustation pattern from the other strains used in our study, because there is a very dense layer visible around the cells (Fig. 4C and D). The iron mineral particles bound to the EPS are much smaller than the minerals surrounding the *Paracoccus* strains (Fig. 4E to H) and may be a result of a difference in EPS composition and/or density, either binding Fe(III) more strongly or in larger amounts. A denser EPS layer could also decrease diffusion of nitrate and nitrite, explaining the slower and incomplete nitrate consumption by strain 2002 (Fig. 1B).

Investigating wet samples of BoFeN1 by CLSM showed that larger amounts of EPS were produced when the strain was cultured in the presence of Fe(II) than in the absence of Fe(II) (Fig. 6; also, see Fig. S4 in the supplemental material), suggesting that the EPS could be produced in order to lower the toxicity of Fe^{2+}. It is worth noting, though, that we cannot exclude the possibility that EPS with a different chemical composition was produced and present but could not be stained with the lectin WGA. Nevertheless, EPS, which is typically composed of protein and mainly polysaccharide polymers, is often produced by cells in response to the presence of toxic chemicals (57). Several studies showed that EPS production is enhanced in the presence of toxic metals such as cadmium and copper (58, 59) and functions as a protective barrier. The binding of several metals, including iron, was shown for bacterial EPS (60–63). Fe^{2+} is known to be toxic due to the formation of oxygen radicals in the Fenton reaction under oxic conditions (64). There are only a few studies concerning the toxicity of Fe^{2+} under anoxic conditions (65, 66). Some nitrate-reducing Fe(II)-oxidizing strains are not able to grow on dissolved Fe(II) but instead require chelated Fe(II), for example, *Paracoccus ferrooxidans* (41) and *Pseudogulbenkiania* strain MAI-1 (67), and it was suggested by those authors that this was due to Fe^{2+} toxicity. Whether these strains cannot produce EPS in the presence of toxic Fe(II), and whether this is the reason for the absence of Fe(II) oxidation, is currently unknown.

Cell encrustation by Fe(II) oxidation via nitrite. The fact that heterotrophic denitrifiers become encrusted in a way similar to that described before for the nitrate-reducing Fe(II) oxidizer BoFeN1 suggests the possibility of abiotic Fe(II) oxidation and cell encrustation by biologically produced nitrite for nitrate-reducing strains under heterotrophic growth conditions (Fig. 7). Nitrite and NO are present in the periplasm during denitrification with electrons stemming from oxidation of organic carbon (68) and can react abiotically with dissolved or solid-phase Fe(II) to Fe(III) (29, 48), leading to Fe(III) mineral precipitation. In the case of BoFeN1, the Fe(III) mineral precipitation starts in the periplasm, continues on the cell surface, and then terminates in the cytoplasm (13). In all cultures, mineral precipitation at the cell surface was probably initially avoided by a protective EPS layer surrounding the cells, which potentially complexed Fe(III) and/or inhibited crystal nucleation and crystal growth because of binding of Fe ions by the organics (55). When nitrite diffuses through this EPS layer, green rust and goethite minerals form on the outside of the EPS layer, catalyzing Fe(II) oxidation and Fe(III) mineral formation (31, 46, 69). This mechanism would also explain the observations of (i) Fe(III) mineral formation without direct contact with the cells despite the low solubility of Fe(III) (14), (ii) oxidation of Fe(II) by sterile-filtered supernatants (67), and (iii) formation of an Fe(III) mineral coating on *Shewanella putrefaciens* cells incubated with Fe^{2+} and NO_2^- (69).

Is cell encrustation deleterious? To determine whether cultures are actually dead after Fe(II) oxidation accompanied by encrustation of all cells, we monitored consumption of acetate from solution as a measure for bacterial activity. We found that all four

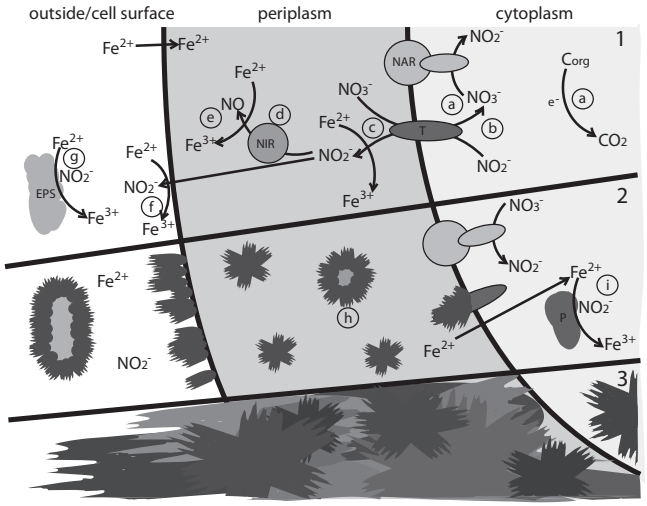

FIG 7 Proposed nitrite-driven mechanism of encrustation during heterotrophic denitrification in an Fe(II)-rich environment. For simplicity, only the first three enzymes of the denitrification pathway are shown. (Phase 1) Nitrate reduction by nitrate reductase (NAR) to nitrite with electrons stemming from organic carbon oxidation (a) and nitrite transport out of the cytoplasm to the periplasm by a transporter (there is also the possibility of separate nitrate/nitrite transporters) (T) (b), leading to an accumulation of nitrite in the periplasm (c) and outside the cell (f). Nitrite is further reduced by the periplasmic nitrite reductase (NIR) to NO (d). There is also possible oxidation of dissolved Fe(II) by nitrite or NO (c, e, f, and g), forming Fe(III), which will rapidly hydrolyze and precipitate as Fe(II)/Fe(III) minerals, such as green rust, and Fe(III) minerals, such as goethite. (Phase 2) Parts of the periplasm and enzymes become encrusted (h). As soon as nitrite transport and/or the periplasm is blocked by minerals, nitrite accumulates inside the cell (i), thus leading to Fe(III) mineral formation inside the cell. (Phase 3) Fe(III) minerals have filled the periplasm and the inside of the cell, probably leading to cell death. Minerals have also grown at the cell surface and associated with the EPS.

strains tested were able to consume acetate even at a late stage of Fe(II) oxidation, when many, or even most, of the cells were encrusted with Fe(III) minerals. This observation might have several explanations. First, there is the possibility that some encrusted cells could grow out of, or discard, the encrustation and resume metabolic activity; this has been demonstrated previously with the formation of gypsum on cyanobacteria (70). Second, encrusted cells might still be able to consume some acetate despite encrustation. Third, there may have been some nonencrusted and thus metabolically healthy and active cells in the cultures.

When the maximum acetate consumption rate of 2.9 ± 0.5 mM/day for strain BoFeN1 in the beginning of the experiment (first acetate amendment) is compared to the rate observed when acetate was added after complete Fe(II) oxidation (1.6 ± 0.05 mM/day), and considering cell numbers published by Muehe et al. (40) (inoculum of 5E + 06 cells/ml and final cell number of 1.2E + 08 cells/ml), it is clear that if only ~2% of the cells present at the end of Fe(II) oxidation remained metabolically active, they could be responsible for the measured acetate consumption rates. When analyzing samples from BoFeN1 and ATCC 19367 after complete Fe(II) oxidation by SEM and CLSM, we indeed detected low numbers of nonencrusted cells. This is supported by the presence of living cells at the end of Fe(II) oxidation, demonstrated by dead-live staining by Kappler et al. (10). As the samples were centrifuged for microscopy analysis, it is possible that due to the higher density of iron minerals, the pellets were enriched in encrusted cells and the actual number of nonencrusted cells in the cultures might have been even higher. To confirm viability, we tested samples from fully oxidized cultures for aerobic growth on LB plates (data not shown) and found that all four strains formed colonies and grew, although both *Paracoccus* strains showed only very poor growth and BoFeN1 and 2002 showed diminished growth. Nevertheless, this suggests that a fraction of cells are indeed not encrusted even at a late stage of oxidation and are able to continue metabolizing acetate and nitrate, whereas the rest of the culture is probably dead. This is underlined by the fact that we saw DNA-free, encrusted cells in BoFeN1 cultures, indicating cell lysis (see Fig. S3 in the supplemental material). Chakraborty and Picardal (71) did similar experiments with a newly isolated *Dechloromonas* strain which was, however, not able to metabolize acetate that was added after complete Fe(II) oxidation. Whether the formation of EPS in the strains we tested protected at least some of the cells sufficiently to survive Fe(III) formation, whether the lower concentration of acetate in their study led to the absence of nonencrusted or lightly encrusted and thus still metabolically active cells, or whether there is another reason for this difference remains unclear. Based on our data, it seems that at least a certain fraction of cells of nitrate-reducing bacteria found a way to survive encrustation in the Fe(II)-rich cultures.

Environmental significance and implications for preservation and mineral studies. Our study suggests that the Fe(III) minerals encrusting the nitrate reducers are probably a metabolic by-product of heterotrophic nitrite formation. Partly and fully mineralized cells have been detected in Fe(II)-rich rivers and springs (72, 73), even with the very unique formation of a layer rich in iron and organic material, similar to the ones observed in our study (Fig. 5B; also, see the supplemental material) (74). We would like to note, however, that the similarity of encrustation patterns observed in the environment to the structures observed with the four strains used in our study has to be interpreted with caution, because in contrast to our study, most TEM studies use heavy metal stains, such as uranyl acetate and lead citrate. These heavy metals are adsorbed by functional groups of biological structures and thus generate similar contrast even without iron being present. Because nitrate reduction is a very widespread microbial metabolism, the observed Fe(II) oxidation by normal denitrifiers has implications for cultivation-based studies focusing on quantification and isolation of nitrate-reducing Fe(II) oxidizers from the environment, since normal denitrifiers will also be recognized and counted as Fe(II) oxidizers in such experiments when additional organic electron donors are added. Furthermore, the encrustation and preservation of denitrifying cells by Fe(III) minerals is of importance, since there are many studies focusing on the preservation of microbial cells as biosignatures or microfossils to draw conclusions about the presence of microbial activity in modern and ancient environments (51, 75–77). And finally, the formation of biogenic iron minerals as a microbial by-product of denitrification also affects other geochemical cycles in nature. Biogenically produced Fe(III) (oxyhydr)oxides are highly reactive toward other metal(loid)s, such as arsenic and uranium, organic pollutants (5, 6, 25, 45), and nutrients such as phosphate (78). The abiotically driven formation of Fe(III) (oxyhydr)oxide minerals by nitrite that is produced by nitrate-reducing bacteria shows that under specific conditions, these very abundant bacteria may influence and facilitate immobilization and transformation of organic and inorganic pollutants, which until now were often mainly attributed to specific Fe(II) oxidizers and Fe(III) reducers (79). The fact that denitrifying bacteria are also able

to cause Fe(II) oxidation will help us to better understand anaerobic Fe(II) oxidation in the environment.

ACKNOWLEDGMENTS

We thank Ellen Struve for HPLC and Marc Zelder for nitrate/nitrite measurements. James Byrne and Christoph Berthold are acknowledged for XRD analyses. We also thank Sebastian Kopf for providing the *Paracoccus* strains.

This work was supported by a research grant from the German Research Foundation (DFG) to A.K., by the Emmy-Noether program of the DFG to M.O. (OB 362/1-1), and by the Natural Sciences and Engineering Research Council of Canada (NSERC) to K.O.K.

REFERENCES

1. **Kappler A, Straub KL.** 2005. Geomicrobiological cycling of iron. Rev. Mineral. Geochem. **59:**85–108. http://dx.doi.org/10.2138/rmg.2005.59.5.
2. **Hedrich S, Schlomann M, Johnson DB.** 2011. The iron-oxidizing proteobacteria. Microbiology **157:**1551–1564. http://dx.doi.org/10.1099/mic.0.045344-0.
3. **Kendall B, Anbar AD, Kappler A, Konhauser KO.** 2012. The global iron cycle, p 65–92. *In* Knoll AH, Canfield DE, Konhauser KO (ed), Fundamentals of geobiology. John Wiley and Sons, Ltd., New York, NY.
4. **Konhauser KO, Kappler A, Roden EE.** 2011. Iron in microbial metabolisms. Elements **7:**89–93. http://dx.doi.org/10.2113/gselements.7.2.89.
5. **Vaughan DJ, Lloyd JR.** 2011. Mineral-organic-microbe interactions: environmental impacts from molecular to macroscopic scales. C. R. Geosci. **343:**140–159. http://dx.doi.org/10.1016/j.crte.2010.10.005.
6. **Borch T, Kretzschmar R, Kappler A, Van Cappellen P, Ginder-Vogel M, Voegelin A, Campbell K.** 2010. Biogeochemical redox processes and their impact on contaminant dynamics. Environ. Sci. Technol. **44:**15–23. http://dx.doi.org/10.1021/es9026248.
7. **Clarke WA, Konhauser KO, Thomas JC, Bottrell SH.** 1997. Ferric hydroxide and ferric hydroxysulfate precipitation by bacteria in an acid mine drainage lagoon. FEMS Microbiol. Rev. **20:**351–361. http://dx.doi.org/10.1111/j.1574-6976.1997.tb00320.x.
8. **Straub KL, Benz M, Schink B, Widdel F.** 1996. Anaerobic, nitrate-dependent microbial oxidation of ferrous iron. Appl. Environ. Microbiol. **62:**1458–1460.
9. **Benz M, Brune A, Schink B.** 1998. Anaerobic and aerobic oxidation of ferrous iron at neutral pH by chemoheterotrophic nitrate-reducing bacteria. Arch. Microbiol. **169:**159–165. http://dx.doi.org/10.1007/s002030050555.
10. **Kappler A, Schink B, Newman DK.** 2005. Fe(III) mineral formation and cell encrustation by the nitrate-dependent Fe(II) oxidizer strain BoFeN1. Geobiology **3:**235–245. http://dx.doi.org/10.1111/j.1472-4669.2006.00056.x.
11. **Weber KA, Pollock J, Cole KA, O'Connor SM, Achenbach LA, Coates JD.** 2006. Anaerobic nitrate-dependent iron(II) bio-oxidation by a novel lithoautotrophic betaproteobacterium, strain 2002. Appl. Environ. Microbiol. **72:**686–694. http://dx.doi.org/10.1128/AEM.72.1.686-694.2006.
12. **Chakraborty A, Roden EE, Schieber J, Picardal F.** 2011. Enhanced growth of *Acidovorax* sp. strain 2AN during nitrate-dependent Fe(II) oxidation in batch and continuous-flow systems. Appl. Environ. Microbiol. **77:**8548–8556. http://dx.doi.org/10.1128/AEM.06214-11.
13. **Miot J, Maclellan K, Benzerara K, Boisset N.** 2011. Preservation of protein globules and peptidoglycan in the mineralized cell wall of nitrate-reducing, iron(II)-oxidizing bacteria: a cryo-electron microscopy study. Geobiology **9:**459–470. http://dx.doi.org/10.1111/j.1472-4669.2011.00298.x.
14. **Miot J, Benzerara K, Morin G, Kappler A, Bernard S, Obst M, Ferard C, Skouri-Panet F, Guigner JM, Posth N, Galvez M, Brown GE, Guyot F.** 2009. Iron biomineralization by anaerobic neutrophilic iron-oxidizing bacteria. Geochim. Cosmochim. Acta **73:**696–711. http://dx.doi.org/10.1016/j.gca.2008.10.033.
15. **Schaedler S, Burkhardt C, Hegler F, Straub KL, Miot J, Benzerara K, Kappler A.** 2009. Formation of cell-iron-mineral aggregates by phototrophic and nitrate-reducing anaerobic Fe(II)-oxidizing bacteria. Geomicrobiol. J. **26:**93–103. http://dx.doi.org/10.1080/01490450802660573.
16. **Hegler F, Schmidt C, Schwarz H, Kappler A.** 2010. Does a low-pH microenvironment around phototrophic FeII-oxidizing bacteria prevent cell encrustation by FeIII minerals? FEMS Microbiol. Ecol. **74:**592–600. http://dx.doi.org/10.1111/j.1574-6941.2010.00975.x.
17. **Chan CS, Fakra SC, Edwards DC, Emerson D, Banfield JF.** 2009. Iron oxyhydroxide mineralization on microbial extracellular polysaccharides. Geochim. Cosmochim. Acta **73:**3807–3818. http://dx.doi.org/10.1016/j.gca.2009.02.036.
18. **Chan CS, Fakra SC, Emerson D, Fleming EJ, Edwards KJ.** 2011. Lithotrophic iron-oxidizing bacteria produce organic stalks to control mineral growth: implications for biosignature formation. ISME J. **5:**717–727. http://dx.doi.org/10.1038/ismej.2010.173.
19. **Comolli LR, Luef B, Chan CS.** 2011. High-resolution 2D and 3D cryo-TEM reveals structural adaptations of two stalk-forming bacteria to an Fe-oxidizing lifestyle. Environ. Microbiol. **13:**2915–2929. http://dx.doi.org/10.1111/j.1462-2920.2011.02567.x.
20. **Miot J, Benzerara K, Obst M, Kappler A, Hegler F, Schadler S, Bouchez C, Guyot F, Morin G.** 2009. Extracellular iron biomineralization by photoautotrophic iron-oxidizing bacteria. Appl. Environ. Microbiol. **75:**5586–5591. http://dx.doi.org/10.1128/AEM.00490-09.
21. **Saini G, Chan CS.** 2013. Near-neutral surface charge and hydrophilicity prevent mineral encrustation of Fe-oxidizing micro-organisms. Geobiology **11:**191–200. http://dx.doi.org/10.1111/gbi.12021.
22. **Kappler A, Newman DK.** 2004. Formation of Fe(III)-minerals by Fe(II)-oxidizing photoautotrophic bacteria. Geochim. Cosmochim. Acta **68:**1217–1226. http://dx.doi.org/10.1016/j.gca.2003.09.006.
23. **Chakraborty A, Picardal F.** 2013. Induction of nitrate-dependent Fe(II) oxidation by Fe(II) in *Dechloromonas* sp. strain UWNR4 and *Acidovorax* sp. strain 2AN. Appl. Environ. Microbiol. **79:**748–752. http://dx.doi.org/10.1128/AEM.02709-12.
24. **Miot J, Benzerara K, Morin G, Bernard S, Beyssac O, Larquet E, Kappler A, Guyot F.** 2009. Transformation of vivianite by anaerobic nitrate-reducing iron-oxidizing bacteria. Geobiology **7:**373–384. http://dx.doi.org/10.1111/j.1472-4669.2009.00203.x.
25. **Hitchcock AP, Obst M, Wang J, Lu YS, Tyliszczak T.** 2012. Advances in the detection of As in environmental samples using low energy X-ray fluorescence in a scanning transmission X-ray microscope: arsenic immobilization by an Fe(II)-oxidizing freshwater bacteria. Environ. Sci. Technol. **46:**2821–2829. http://dx.doi.org/10.1021/es202238k.
26. **Melton ED, Schmidt C, Kappler A.** 2012. Microbial iron(II) oxidation in littoral freshwater lake sediment: the potential for competition between phototrophic vs. nitrate-reducing iron(II) oxidizers. Front. Microbiol. **3:**197. http://dx.doi.org/10.3389/fmicb.2012.00197.
27. **Van Cleemput O, Samater AH.** 1996. Nitrite in soils: accumulation and role in the formation of gaseous N compounds. Fert. Res. **45:**81–89.
28. **Nelson DW, Bremner JM.** 1970. Role of soil minerals and metallic cations in nitrite decomposition and chemo-denitrification in soils. Soil Biol. Biochem. **2:**1–8. http://dx.doi.org/10.1016/0038-0717(70)90019-2.
29. **Bonner FT, Pearsall KA.** 1982. Aqueous nitrosyliron(I1) chemistry. 1. Reduction of nitrite and nitric oxide by iron(I1) and (trioxodinitrato)iron(II) in acetate buffer. intermediacy of nitrosyl hydride. Inorg. Chem. **21:**1973–1978.
30. **Picardal F.** 2012. Abiotic and microbial interactions during anaerobic transformations of Fe(II) and NOx-. Front. Microbiol. **3:**112. http://dx.doi.org/10.3389/fmicb.2012.00112.
31. **Klueglein N, Kappler A.** 2013. Abiotic oxidation of Fe(II) by reactive nitrogen species in cultures of the nitrate-reducing Fe(II) oxidizer Acidovorax sp. BoFeN1—questioning the existence of enzymatic Fe(II) oxidation. Geobiology **11:**180–190. http://dx.doi.org/10.1111/gbi.12019.
32. **Rosch C, Mergel A, Bothe H.** 2002. Biodiversity of denitrifying and dinitrogen-fixing bacteria in an acid forest soil. Appl. Environ. Microbiol. **68:**3818–3829. http://dx.doi.org/10.1128/AEM.68.8.3818-3829.2002.
33. **Weber KA, Hedrick DB, Peacock AD, Thrash JC, White DC, Achenbach LA, Coates JD.** 2009. Physiological and taxonomic description of the novel autotrophic, metal oxidizing bacterium, Pseudogulbenkiania sp strain 2002. Appl. Microbiol. Biotechnol. **83:**555–565. http://dx.doi.org/10.1007/s00253-009-1934-7.
34. **Vries G, Harms N, Hoogendijk J, Stouthamer A.** 1989. Isolation and characterization of *Paracoccus denitrificans* mutants with increased conjugation frequencies and pleiotropic loss of a (nGATCn) DNA-modifying property. Arch. Microbiol. **152:**52–57. http://dx.doi.org/10.1007/BF00447011.
35. **Carlson CA, Ingraham JL.** 1983. Comparison of denitrification by *Pseudomonas stutzeri*, *Pseudomonas aeruginosa*, and *Paracoccus denitrificans*. Appl. Environ. Microbiol. **45:**1247–1253.
36. **Rainey FA, Kelly DP, Stackebrandt E, Burghardt J, Hiraishi A, Katayama Y, Wood AP.** 1999. A re-evaluation of the taxonomy of *Paracoccus denitrificans* and a proposal for the combination *Paracoccus pantotrophus* comb. nov. Int. J. Syst. Bacteriol. **2:**645–651.
37. **Hegler F, Posth NR, Jiang J, Kappler A.** 2008. Physiology of pho-

totrophic iron(II)-oxidizing bacteria: implications for modern and ancient environments. FEMS Microbiol. Ecol. **66:**250–260. http://dx.doi.org/10.1111/j.1574-6941.2008.00592.x.
38. **Berthold C, Bjeoumikhov A, Bruegamann L.** 2009. Fast XRD2 microdiffraction with focusing X-ray microlenses. Part. Part. Syst. Charact. **26:**107–111. http://dx.doi.org/10.1002/ppsc.200800038.
39. **Lawrence JR, Swerhone GDW, Kuhlicke U, Neu TR.** 2007. In situ evidence for microdomains in the polymer matrix of bacterial microcolonies. Can. J. Microbiol. **53:**450–458. http://dx.doi.org/10.1139/W06-146.
40. **Muehe EM, Gerhardt S, Schink B, Kappler A.** 2009. Ecophysiology and the energetic benefit of mixotrophic Fe(II) oxidation by various strains of nitrate-reducing bacteria. FEMS Microbiol. Ecol. **70:**335–343. http://dx.doi.org/10.1111/j.1574-6941.2009.00755.x.
41. **Kumaraswamy R, Sjollema K, Kuenen G, van Loosdrecht M, Muyzer G.** 2006. Nitrate-dependent Fe(II)EDTA (2-) oxidation by *Paracoccus ferrooxidans* sp nov., isolated from a denitrifying bioreactor. Syst. Appl. Microbiol. **29:**276–286. http://dx.doi.org/10.1016/j.syapm.2005.08.001.
42. **Sorensen J, Thorling L.** 1991. Stimulation by lepidocrocite (γ-FeOOH) of Fe(II)-dependent nitrite reduction. Geochim. Cosmochim. Acta **55:**1289–1294. http://dx.doi.org/10.1016/0016-7037(91)90307-Q.
43. **Wullstein LH, Gilmour CM.** 1966. Non-enzymatic formation of nitrogen gas. Nature **210:**1150–1151. http://dx.doi.org/10.1038/2101150a0.
44. **Van Cleemput O, Baert L.** 1983. Nitrite stability influenced by iron compounds. Soil Biol. Biochem. **15:**137–140. http://dx.doi.org/10.1016/0038-0717(83)90093-7.
45. **Weber KA, Picardal FW, Roden EE.** 2001. Microbially catalyzed nitrate-dependent oxidation of biogenic solid-phase Fe(II) compounds. Environ. Sci. Technol. **35:**1644–1650. http://dx.doi.org/10.1021/es0016598.
46. **Pantke C, Obst M, Benzerara K, Morin G, Ona-Nguema G, Dippon U, Kappler A.** 2012. Green rust formation during Fe(II) oxidation by the nitrate-reducing *Acidovorax* sp. strain BoFeN1. Environ. Sci. Technol. **46:**1439–1446. http://dx.doi.org/10.1021/es2016457.
47. **Hansen HCB, Borggaard OK, Sorensen J.** 1994. Evaluation of the free-energy of formation of Fe(II)-Fe(III) hydroxide-sulfate (green rust) and its reduction by nitrite. Geochim. Cosmochim. Acta **58:**2599–2608. http://dx.doi.org/10.1016/0016-7037(94)90131-7.
48. **Tai YL, Dempsey BA.** 2009. Nitrite reduction with hydrous ferric oxide and Fe(II): stoichiometry, rate, and mechanism. Water Res. **43:**546–552. http://dx.doi.org/10.1016/j.watres.2008.10.055.
49. **Kampschreur MJ, Kleerebezem R, de Vet WWJM, van Loosdrecht MCM.** 2011. Reduced iron induced nitric oxide and nitrous oxide emission. Water Res. **45:**5945–5952. http://dx.doi.org/10.1016/j.watres.2011.08.056.
50. **Carlson HK, Clark IC, Blazewicz SJ, Iavarone AT, Coates JD.** 2013. Fe(II) oxidation is an innate capability of nitrate-reducing bacteria that involves abiotic and biotic reactions. J. Bacteriol. **195:**3260–3268. http://dx.doi.org/10.1128/JB.00058-13.
51. **Glasauer S, Mattes A, Gehring A.** 2013. Constraints on the preservation of ferriferous microfossils. Geomicrobiol. J. **30:**479–489. http://dx.doi.org/10.1080/01490451.2012.718408.
52. **Cornell RM, Schwertmann U.** 2003. The iron oxides: structure, properties, reactions, occurrences and uses, vol 2, p 71. Wiley-VCH, Weinheim, Germany.
53. **Larese-Casanova P, Haderlein SB, Kappler A.** 2010. Biomineralization of lepidocrocite and goethite by nitrate-reducing Fe(II)-oxidizing bacteria: Effect of pH, bicarbonate, phosphate, and humic acids. Geochim. Cosmochim. Acta **74:**3721–3734. http://dx.doi.org/10.1016/j.gca.2010.03.037.
54. **Hauck S, Benz M, Brune A, Schink B.** 2001. Ferrous iron oxidation by denitrifying bacteria in profundal sediments of a deep lake (Lake Constance). FEMS Microbiol. Ecol. **37:**127–134. http://dx.doi.org/10.1111/j.1574-6941.2001.tb00860.x.
55. **Hao L, Li J, Kappler A, Obst M.** 2013. Mapping of heavy metal ion sorption to cell–extracellular polymeric substance–mineral aggregates by using metal-selective fluorescent probes and confocal laser scanning microscopy. Appl. Environ. Microbiol. **79:**6524–6534. http://dx.doi.org/10.1128/AEM.02454-13.
56. **Konhauser KO, Fisher QJ, Fyfe WS, Longstaffe FJ, Powell MA.** 1998. Authigenic mineralization and detrital clay binding by freshwater biofilms: the Brahmani River, India. Geomicrobiol. J. **15:**209–222. http://dx.doi.org/10.1080/01490459809378077.
57. **Aislabie J, Loutit MW.** 1986. Accumulation of Cr(III) by bacteria isolated from polluted sediment. Mar. Environ. Res. **20:**221–232. http://dx.doi.org/10.1016/0141-1136(86)90048-6.
58. **Henriques IDS, Love NG.** 2007. The role of extracellular polymeric substances in the toxicity response of activated sludge bacteria to chemical toxins. Water Res. **41:**4177–4185. http://dx.doi.org/10.1016/j.watres.2007.05.001.
59. **Fang HHP, Xu LC, Chan KY.** 2002. Effects of toxic metals and chemicals on biofilm and biocorrosion. Water Res. **36:**4709–4716. http://dx.doi.org/10.1016/S0043-1354(02)00207-5.
60. **Mikutta R, Baumgärtner A, Schippers A, Haumaier L, Guggenberger G.** 2012. Extracellular polymeric substances from *Bacillus subtilis* associated with minerals modify the extent and rate of heavy metal sorption. Environ. Sci. Technol. **46:**3866–3873. http://dx.doi.org/10.1021/es204471x.
61. **Ferris FG, Schultze S, Witten TC, Fyfe WS, Beveridge TJ.** 1989. Metal interactions with microbial biofilms in acidic and neutral pH environments. Appl. Environ. Microbiol. **55:**1249–1257.
62. **Beveridge TJ, Koval SF.** 1981. Binding of metals to cell envelopes of Escherichia coli K-12. Appl. Environ. Microbiol. **42:**325–335.
63. **Konhauser KO, Urrutia MM.** 1999. Bacterial clay authigenesis: a common biogeochemical process. Chem. Geol. **161:**399–413. http://dx.doi.org/10.1016/S0009-2541(99)00118-7.
64. **Cornelis P, Wei Q, Andrews SC, Vinckx T.** 2011. Iron homeostasis and management of oxidative stress response in bacteria. Metallomics **3:**540–549. http://dx.doi.org/10.1039/c1mt00022e.
65. **Bird LJ, Coleman ML, Newman DK.** 2013. Iron and copper act synergistically to delay anaerobic growth of bacteria. Appl. Environ. Microbiol. **79:**3619–3627. http://dx.doi.org/10.1128/AEM.03944-12.
66. **Poulain AJ, Newman DK.** 2009. *Rhodobacter capsulatus* catalyzes light-dependent Fe(II) oxidation under anaerobic conditions as a potential detoxification mechanism. Appl. Environ. Microbiol. **75:**6639–6646. http://dx.doi.org/10.1128/AEM.00054-09.
67. **Kopf SH, Henny C, Newman DK.** 2013. Ligand-enhanced abiotic iron oxidation and the effects of chemical versus biological iron cycling in anoxic environments. Environ. Sci. Technol. **47:**2602–2611. http://dx.doi.org/10.1021/es3049459.
68. **Philippot L.** 2002. Denitrifying genes in bacterial and archaeal genomes. Biochim. Biophys. Acta **1577:**355–376. http://dx.doi.org/10.1016/S0167-4781(02)00420-7.
69. **Coby AJ, Picardal FW.** 2005. Inhibition of NO3- and NO2- reduction by microbial Fe(III) reduction: Evidence of a reaction between NO2- and cell surface-bound Fe2+. Appl. Environ. Microbiol. **71:**5267–5274. http://dx.doi.org/10.1128/AEM.71.9.5267-5274.2005.
70. **Schultze-Lam S, Harauz G, Beveridge TJ.** 1992. Participation of a cyanobacterial S layer in fine-grained mineral formation. J. Bacteriol. **174:**7971–7981.
71. **Chakraborty A, Picardal F.** 2013. Neutrophilic, nitrate-dependent, Fe(II) oxidation by a *Dechloromonas* species. World J. Microbiol. Biotechnol. **29:**617–623. http://dx.doi.org/10.1007/s11274-012-1217-9.
72. **Benzerara K, Morin G, Yoon TH, Miot J, Tyliszczak T, Casiot C, Bruneel O, Farges F, Brown GE.** 2008. Nanoscale study of As biomineralization in an acid mine drainage system. Geochim. Cosmochim. Acta **72:**3949–3963. http://dx.doi.org/10.1016/j.gca.2008.05.046.
73. **Preston LJ, Shuster J, Fernandez-Remolar D, Banerjee NR, Osinski GR, Southam G.** 2011. The preservation and degradation of filamentous bacteria and biomolecules within iron oxide deposits at Rio Tinto, Spain. Geobiology **9:**233–249. http://dx.doi.org/10.1111/j.1472-4669.2011.00275.x.
74. **Konhauser KO.** 1998. Diversity of bacterial iron mineralization. Earth Sci. Rev. **43:**91–121. http://dx.doi.org/10.1016/S0012-8252(97)00036-6.
75. **Banfield JF, Moreau JW, Chan CS, Welch SA, Little B.** 2001. Mineralogical biosignatures and the search for life on Mars. Astrobiology **1:**447–465. http://dx.doi.org/10.1089/153110701753593856.
76. **Posth NR, Hegler F, Konhauser KO, Kappler A.** 2008. Alternating Si and Fe deposition caused by temperature fluctuations in Precambrian oceans. Nat. Geosci. **1:**703–708. http://dx.doi.org/10.1038/ngeo306.
77. **Cosmidis J, Benzerara K, Gheerbrant E, Esteve I, Bouya B, Amaghzaz M.** 2013. Nanometer-scale characterization of exceptionally preserved bacterial fossils in Paleocene phosphorites from Ouled Abdoun (Morocco). Geobiology **11:**139–153. http://dx.doi.org/10.1111/gbi.12022.
78. **Konhauser KO, Fyfe WS, Schultzelam S, Ferris FG, Beveridge TJ.** 1994. Iron phosphate precipitation by epilithic microbial biofilms in arctic Canada. Can. J. Earth. Sci. **31:**1320–1324. http://dx.doi.org/10.1139/e94-114.
79. **Hohmann C, Morin G, Ona-Nguema G, Guigner J-M, Brown GE, Jr, Kappler A.** 2011. Molecular-level modes of As binding to Fe(III) (oxyhydr)oxides precipitated by the anaerobic nitrate-reducing Fe(II)-oxidizing Acidovorax sp strain BoFeN1. Geochim. Cosmochim. Acta **75:**4699–4712. http://dx.doi.org/10.1016/j.gca.2011.02.044.